

Cargo Transport by Teams of Molecular Motors: Basic Mechanisms for Intracellular Drug Delivery

MELANIE J. I. MÜLLER, FLORIAN BERGER, STEFAN KLUMPP, and REINHARD LIPOWSKY

Department of Theory & Bio-Systems, Max Planck Institute of Colloids and Interfaces, Potsdam, Germany

16.1 INTRODUCTION

16.1.1 Barriers to Gene Therapy and Drug Delivery

The delivery of drug carriers or viral and nonviral vectors for gene therapy is hampered by many extracellular and intracellular barriers. The drug or DNA carrier must find its way from the injection site to the target cell, avoiding sequestration and destruction, for example, by cells of the immune system. Upon reaching the target cell, the carrier must pass the plasma membrane to enter the cell, traverse the cytoplasm to its intracellular destination, possibly enter a target organelle like the nucleus or a mitochondrion, and then perform its function. Traditionally, research has focused on overcoming membrane barriers: how to get the drug carriers or transfection vectors into the cell and, once inside the cell, how to get these particles into the target organelle. However, the cytoplasm itself is also a major obstacle to delivery, especially for nonviral gene therapy: After a transfection vector has been released into the cytoplasm, it may have difficulties reaching the nucleus [1, 2].

16.1.2 Inefficient Transport Via Diffusion

One fact that is often overlooked is that drug or gene carriers are too large to diffuse through the cytoplasm at a reasonable rate. The cytoplasm is a crowded,

viscous medium consisting of proteins, filament meshworks, and organelles, which limit the diffusion of large particles [3]. For example, using experimentally determined cytoplasmic diffusion coefficients of DNA [4], a 1000-bp DNA needs about 30 min to diffuse a distance of 10 μm , compared to about 18 s in water. DNA strands that are larger than 2000 bp are practically immobile in the cytoplasm. Gene vectors used in gene transfer have typically several thousand base pairs. Consequently, microinjected plasmids do not diffuse far from their site of injection [5], and transfection increases dramatically if DNA is microinjected into or very close to the nucleus instead of a cytoplasmic location far from the nucleus [5, 6]. Therefore efficient transport to the nucleus cannot be achieved by diffusion and requires an active mechanism.

16.1.3 Viruses as Hijackers

Some viruses face barriers similar to gene therapy: they must enter the host cell and deliver their genetic material to the nucleus. Many viruses have solved the problem of intracellular transport by hijacking the host cell's active transport system [2, 7, 8], as shown in Figure 16.1A. After entering the cell via endocytosis or membrane fusion, the virus particle recruits molecular motors, which act as cellular "nanotrucks" and pull the virus along microtubule filaments toward the nucleus. Similarly, when leaving the cell, the virus uses molecular motors to travel from the site of assembly to the cell membrane. This active transport allows the virus to travel at a velocity of about 1 $\mu\text{m/s}$ [8,

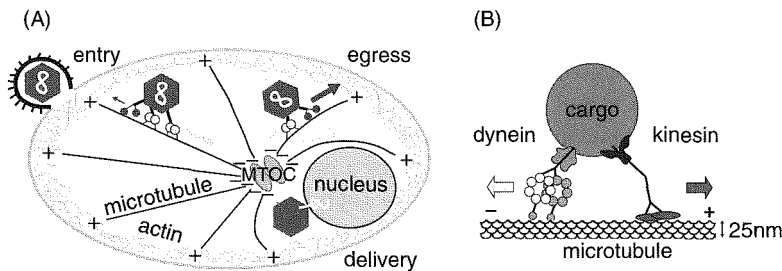


Figure 16.1. Intracellular trafficking. (A) Microtubule filaments (black) form long "highways" from the microtubule-organizing center (MTOC) near the nucleus to the cell periphery, while a dense meshwork of actin filaments (cyan) provides "side roads" for short-range traffic. Plus-end directed (blue) and minus-end directed (yellow) molecular motors pull various cellular cargoes along these filaments. Viruses hijack the cellular transport machinery: after entry into the cell, a virus particle (red) recruits motors from the cytoplasm to travel along microtubules toward the nucleus, where it delivers its genetic material (white). In order to leave the cell, the newly assembled virus uses motors to travel back to the plasma membrane. (B) Cargo particle (red) that is transported along a microtubule by one kinesin-1 (blue) and one cytoplasmic dynein (yellow) motor. (See color insert.)

9] so that it can overcome a distance of $10\mu\text{m}$ in about 10s. For comparison, diffusion of a 100-nm virus capsid in the cytoplasm over the same distance would take a few hours.

16.1.4 Understanding Intracellular Transport

Hijacking the cellular transport machinery is an elegant solution to the problem of transport through the crowded cytoplasm, which is employed by many viruses, such as human immunodeficiency virus, herpes simplex virus, and adenoviruses [2, 7, 8]. These viruses are commonly used in viral gene therapy, in which the gene vector is packaged into a virus capsid. However, also non-viral vectors and drug carriers can bind to molecular motors via adaptor proteins recruited from the cytoplasm, and then travel actively along microtubule filaments [2]. In order to improve gene and drug delivery, it is therefore essential to design carrier systems that can recruit the cellular transport machinery in an appropriate way. As a prerequisite for such a design, a good understanding of intracellular transport by molecular motors is required.

16.1.5 Overview

This chapter is organized as follows. The basic features of molecular motors and cytoskeletal filaments are briefly described in Section 16.2.1. The challenges encountered by motor transport are summarized in Section 16.2.2. The different mechanisms for cooperative transport by motor teams are discussed in Section 16.3. In this latter section, we will distinguish three such mechanisms that we have recently elucidated by the construction and analysis of explicit theoretical models: (1) cargo transport by one team of identical motors [10, 11]; (2) transport by two antagonistic teams of motors that both work on the same type of filament [12, 13]; and (3) cargo transport by two teams of motors that work on different filaments [14]. At the end, we give a brief outlook on open questions and possible applications of the teamwork of molecular motors.

16.2 INTRACELLULAR TRAFFIC OF MOLECULAR MOTORS

16.2.1 Molecular Motors and Their Tracks

The complex internal structure of cells depends to a large extent on active transport: vesicles, as well as RNA, filaments, and protein complexes, move between different compartments, travel from the cell center to the cell periphery or vice versa [15]. This active transport is mainly accomplished by molecular motors. These molecular motors can be compared to road trucks: they travel along a “road network” consisting of cytoskeletal filaments and consume ATP as molecular “fuel.”

16.2.1.1 Cytoskeletal Filaments The road network for the molecular motors is formed by the cytoskeleton. The cytoskeleton is a meshwork built up from three types of filaments—microtubule, actin, and intermediate filaments—which form a complex meshwork throughout the cell. Only microtubules and actin filaments are used in motor transport. Kinesin and dynein motors walk on microtubules, while myosin motors travel along actin filaments. The microtubules form a very structured network spanning the whole cell from the center to the periphery, see Figure 16.1A, and serve as “highways” for the long-range traffic. The actin filaments, on the other hand, form a dense meshwork concentrated near the cell cortex and serve as “side-roads” for short-range traffic. Both types of filaments are polar: their building blocks are asymmetric so that each filament possesses an intrinsic directionality. Each filament has a “plus end,” at which it polymerizes faster than at its “minus end.”

16.2.1.2 Cytoskeletal Motors Each cytoskeletal motor works on a certain filament and recognizes the polarity of this filament. Thus each motor walks either to the filament’s “plus” or “minus” end. The cytoplasmic dynein motor, for example, walks to the microtubule minus end, while the kinesin-1 motor walks to the microtubule plus end; see Figure 16.1B.

16.2.1.3 Kinesin-1 The best-studied motor, kinesin-1, was first identified in the 1980s in a biochemical fractionation of squid axonal tissue [16, 17]. It is a heterotetramer composed of two identical heavy chains and two identical light chains [18]. The heavy chains dimerize to form an α -helical coiled-coil stalk. Each of the 120-kDa heavy chains includes a globular “head” at its N terminus, with both a microtubule-binding domain and an ATP-binding domain. The two heads perform the actual motor activity of the protein. The light chains associate with the heavy chains near the C terminus and form the motor tail, which is involved in cargo binding.

16.2.1.4 Kinesin Stepping When traveling along a microtubule, kinesin-1 rather “steps” than “drives” [19]. A microtubule filament consists of 13 protofilaments aligned in parallel, each of which provides a track for the motor with a binding site every 8 nm. For each step, kinesin moves the trailing head forward to the next binding site in front, while the other head remains bound to the microtubule. In this so-called hand-over-hand mechanism, each head covers a distance of 16 nm, while the center-of-mass of the motor makes a forward step of 8 nm. During each step, the motor hydrolyzes a single ATP molecule.

16.2.1.5 Cytoplasmic Dynein The structure of cytoplasmic dynein, which was discovered as a minus end microtubule motor in the 1980s [20], is more complex than that of kinesin [18, 21], as indicated in Figure 16.1B. Dynein also has two heads, which can bind to the microtubule, but its ATP-binding

domains reside in rings of seven globular domains, which are connected to the heads by a short coiled-coil stalk. Several light and intermediate chains are attached near the cargo binding end of dynein and are involved in the binding of cargo and of accessory proteins, making dynein a huge multisubunit protein of 1.2MDa.

16.2.1.6 Other Types of Motors Kinesin-1 and cytoplasmic dynein are the most prominent members of a whole “zoo” of molecular motors, consisting of three motor families—kinesins, dyneins, and myosins—as reviewed in Refs. 18, 22, and 23. While the dynein family consists of only two subclasses, the kinesin family has more than ten subclasses. All dyneins walk to the microtubule minus end, whereas most kinesins walk to the microtubule plus end. Several classes of myosins mediate transport on actin filaments.

16.2.2 Challenges for Motor Transport

The various motors described in the last section provide a versatile toolbox for intracellular traffic [18]. These motors transport an enormous amount of vastly different cargoes through the cell, ranging from endosomes and other types of vesicles to RNAs and filaments as well as to whole organelles such as mitochondria [15]. Each cargo has to recruit the right type of motor and an appropriate motor number in order to be shuttled to the correct destination. In this section, we will discuss how the motors perform these challenging tasks.

16.2.2.1 Motor Processivity Native motor molecules have a linear extension of about 100 nm; see Figure 16.1B. Because of their relatively small size, their motion is strongly affected by thermal fluctuations and viscous forces: molecular motors continuously collide with other molecules and thus walk “in a strong storm.” Because of this thermal noise, molecular motors unbind from their track from time to time. Upon unbinding they lose their ability to perform directed motion and randomly diffuse in the surrounding solution until they finally rebind to a filament. For kinesin-1, unbinding happens on average after a run time of about 1 s, or equivalently a run length (or walking distance) of about 1 μm . A cellular cargo, however, must accomplish distances of tens of micrometers, and in some extremely large cells like neurons even up to a meter [24].

16.2.2.2 Load Forces Molecular motors can generate forces in the range of a few piconewtons [22, 25, 26]. This has to be compared to the frictional force,

$$F_{\text{fr}} = \phi_{\text{fr}} v \quad \text{with} \quad \phi_{\text{fr}} = 6\pi\eta R = k_{\text{B}}T/D \quad (16.1)$$

experienced by the cargo particle of size R as it moves through a medium with dynamical viscosity η . The parameter D is the diffusion coefficient of the

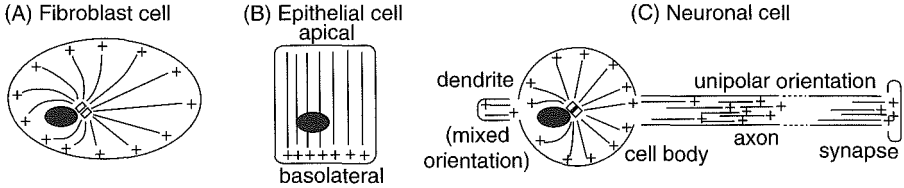


Figure 16.2. Organization of microtubules (black lines with indicated plus ends) in three different cell types for which the nuclei are represented as black ellipses and the microtubule-organizing centers or centrosomes as white rectangles. (A) In fibroblast cells, microtubule minus ends nucleate at the centrosome and the plus ends point radially outwards. (B) In epithelial cells, microtubules form a parallel array with minus ends pointing to the apical and plus ends to the basolateral surface. (C) In long axons of neuron cells, microtubules form an isopolar array with the plus ends oriented toward the synapses at the axon tips.

(unbound) cargo, and $k_B T$ is Boltzmann's constant times absolute temperature. In water with dynamical viscosity $\eta = 1 \text{ mPa} \cdot \text{s}$, the force needed to pull a $1\text{-}\mu\text{m}$ sized cargo at a velocity of $v = 1 \mu\text{m/s}$ is equal to 0.01 pN , which is negligible for a molecular motor that is able to generate several piconewtons of force. However, since diffusion in the cytoplasm is slowed down by a factor of $10\text{--}1000$ depending on the cargo size [47], it follows from Equation 16.1 that frictional forces in the cytoplasm can be in the range of $0.1\text{--}10 \text{ pN}$, which represents a large load for a molecular motor. For these estimates, we assumed that the diffusion coefficient D as measured for cargo diffusion in the cytoplasm also applies to motor transport; see, however, Ref. 27.

16.2.2.3 Bidirectional Transport Cells typically have an “isopolar” microtubule cytoskeleton [28]; see Figure 16.2. In a “round” cell such as a fibroblast cell, for example, microtubules are arranged radially, with their minus ends close to the nucleus at the cell center and their plus ends directed outward to the cell periphery. In epithelial cells, microtubules form a parallel array with their minus ends pointing to the apical and their plus ends to the basolateral surface. The isopolar microtubule arrangement is most pronounced in long cellular subcompartments such as neuronal axons or fungal hyphae. In these long and relatively narrow membrane tubes, the microtubules are arranged parallel to the tube axis with their minus ends pointing to the cell body and the plus ends pointing to the tip.

Single molecular motors walk along these tracks only into one direction: dyneins to the minus ends, and most kinesins to the plus ends. However, many cellular cargoes travel in both directions [29, 30], a transport mode that avoids accumulation of cargo at either the cell periphery or the cell center [31, 32]. Cargoes like endosomes, mitochondria, and viruses are observed to move bidirectionally, reversing direction every few seconds [29, 30]. These cargoes have both plus- and minus-end directed motors attached. Bidirectional

motion can lead to net transport if the runs in one direction are on average longer or faster than runs in the other direction. Therefore bidirectional transport requires an appropriate balance between the activity of plus and minus motors.

16.2.2.4 Transport Regulation Cellular regulation of cargo transport often leads to changes in the run lengths, that is, the distances covered during runs into the plus or the minus direction. This has been observed for the directional regulation of mitochondria in axons [33], of lipid droplets during embryo development [34], of virus targeting during entry and egress [35], and of melanosomes during dispersion and aggregation [36]. In the latter example, melanosome redistribution in specialized pigment cells of fish or frog allows the organism to adapt its skin color to the environment. During “aggregation,” minus-end motion dominates, and the melanosomes accumulate in the cell center. During “dispersion,” the melanosomes spread out over the whole cell because of a decrease in minus run length [36]. Aggregation and dispersion are triggered by hormonal stimulation, which is transmitted to the motors via a signal cascade involving cAMP and protein kinase A (PKA) [37].

16.2.2.5 Transport on Two Types of Tracks Intracellular transport usually proceeds in two steps [38, 39]; see Figure 16.1A. Long-range transport from the cell center to the periphery and vice versa is mediated by kinesins and dyneins walking along the long microtubule highways, while short-range delivery is the task of myosin motors using the dense actin meshwork in the cell cortex. This “dual transport” requires that cargoes are able to switch from microtubule to actin tracks, as has indeed been observed for various cellular cargo such as mitochondria, pigment granules, and synaptic vesicles, reviewed in Refs. 38 and 39. These cargoes need to balance the activities of actin- and microtubule-based motors. A prominent example is again the traffic of melanosomes, which are carried by kinesin-2 and cytoplasmic dynein along microtubules and by myosin V along actin filaments [38]. During dispersion, myosin V is upregulated, which leads to enhanced switching of melanosomes to actin filaments [36, 40]. During aggregation, downregulation of myosin V “recollects” the melanosomes to the microtubules, on which they are then transported toward the cell center.

16.3 TEAMWORK OF MOLECULAR MOTORS

16.3.1 Different Levels of Motor Motility

In general, the behavior of molecular motors involves several levels of motility [41] related to (i) the stepping of single motors, (ii) the cooperative transport of cargo by motor teams, and (iii) the traffic of many motor-propelled cargoes. At the level (i) of a single motor, most progress has been made in understand-

ing the structure and the stepping mechanism of kinesin-1, in particular, the coordination of its two heads [19, 21, 42]. The level (iii) of cell wide cargo trafficking has received mainly theoretical attention. On the cellular length scale, each cargo is viewed in a course-grained manner as a particle with the ability to bind and actively move along cytoskeletal filaments, while diffusing randomly in the surrounding solution. This description allows one to calculate quantities such as the densities and fluxes of cargoes throughout the cell [43–46], which are important to characterize the intracellular traffic. For drug delivery, gene therapy, or virus trafficking, another important quantity is the mean first passage time from the point of entry into the cell to the intracellular target [47, 48].

16.3.2 Motor Teams

The level (ii) of cooperative transport by several molecular motors will be the focus of this chapter. Many cellular cargoes are attached to more than one motor, and to more than one type of motor [29, 30, 38, 39]. The number of motors in a team is small, typically between 1 and 10 [27]. Cargo transport by small teams of molecular motors is a topic of current research both experimentally [27, 49–54] and theoretically [11, 13, 14, 50, 55, 56]. In the following, we will review our recent theoretical studies of cargo transport by small teams of molecular motors [11–14]. After introducing our model for a single motor in the next section, we will first examine the transport by one cooperating team of molecular motors that all belong to the same species. We will then discuss transport by two antagonistic teams of molecular motors that walk into opposite directions, and finally transport by two teams of motors that can walk on different types of filaments.

16.3.3 Transport Properties of a Single Motor

16.3.3.1 Different Subprocesses of Motor Transport Since we are interested in cargo motion on time scales ranging from seconds to minutes and length scales from a few to hundreds of micrometers, we can describe the motors in a coarse-grained manner. We neglect the details of their protein structure and stepping cycle but take their finite binding time to the track into account. The motors exhibit three basic subprocesses: they walk along the filament with velocity v , unbind from this filament with rate ϵ , and rebind to it with rate π ; see Figure 16.3A. If the motor experiences no load force, these parameters are of the order of $\pi_0 \sim 1/s$, $v_f \sim 1 \mu\text{m}/s$, and $\epsilon_0 \sim 1/s$, respectively; see Table 16.1. If the motor has to work against a load force F , both the motor velocity v and its unbinding rate ϵ strongly depend on this force; see Figure 16.3B,C. This force dependence has been investigated experimentally for some motors using optical traps or tweezers. An optical trap uses a focused laser beam, the radiation pressure of which is able to exert forces in the piconewton-range on dielectric objects of nanometer to micrometer size. If a

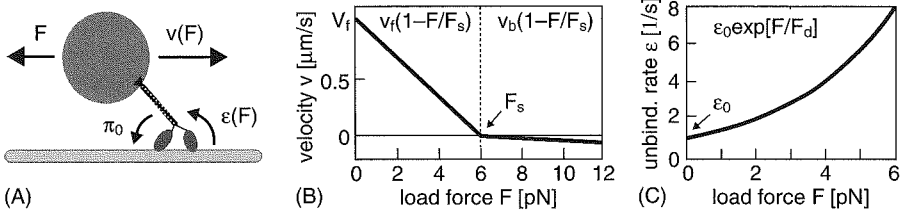


Figure 16.3. Transport properties of a single motor. (A) A single motor walks along the filament with velocity v , unbinds from the filament with rate ϵ , and rebinds to it with rate $\pi = \pi_0$. If the cargo experiences a load force F , both the velocity v and the unbinding rate ϵ depend on F . (B) Motor velocity v as a function of load force F as parameterized in Equations 16.2 and 16.3. The velocity decreases with increasing F until it vanishes at the stall force F_s . For superstall forces $F > F_s$, the motor steps backwards with a relatively small velocity. (C) Motor unbinding rate ϵ as a function of F as in Equation 16.4. The unbinding rate increases exponentially with increasing F . (See color insert.)

TABLE 16.1 Single Motor Parameters for Conventional Kinesin or Kinesin-1 and Cytoplasmic Dynein^a

Parameter	Symbol	Kinesin	Dynein
Stall force	F_s	6 pN [25, 7, 58]	7 pN [26]
Detachment force	F_d	3 pN [59]	3 pN ?
Unbinding rate	ϵ_0	1/s [59]	0.25/s [60]
Binding rate	π_0	5/s [10, 52]	1.5/s [60]
Forward velocity	v_f	1 $\mu\text{m/s}$ [25, 7, 58]	1 $\mu\text{m/s}$ [26, 60]
Backward velocity	v_b	6 nm/s [25, 7]	6 nm/s ?

^aThese are abbreviated here as “kinesin” and “dynein,” respectively. The experimentally determined values for the stall force F_s of kinesin [25, 7, 58] vary between 5.5 pN and 7.6 pN. For dynein, the parameters with a question mark are currently not available from experimental studies; in the latter case, we used the same parameters for dynein as for kinesin.

single motor is bound to such an object, the movement of this motor can be studied under a constant load force F .

16.3.3.2 Single Motor Parameters The results of optical trapping experiments imply that the motor velocity v decreases approximately linearly with force F and is well described by the functional form

$$v(F) = v_f(1 - F/F_s) \quad \text{for } 0 \leq F \leq F_s \quad (16.2)$$

which vanishes at the “stall force” $F = F_s$ [25, 59]. For higher load forces $F > F_s$, the motor walks backwards very slowly [25, 57]; we use the parametrization [13]

$$v(F) = v_b(1 - F/F_s) \quad \text{for } F_s \leq F \quad (16.3)$$

with $v_b \ll v_f$.

The unbinding rate of the motor from the filament increases exponentially with applied force F according to [11]

$$\varepsilon(F) = \varepsilon_0 \exp(|F|/F_d) \quad (16.4)$$

with the detachment force F_d as obtained, for positive F , from the measurements of the walking distance of a single motor as a function of load [59] in agreement with Kramers' rate theory [61]. Such an exponential form has also been used in the context of receptor-ligand binding at membranes [62].

The binding rate of the motor to the microtubule is taken to be independent of the load force and given by [11]

$$\pi(F) = \pi_0 \quad \text{for all } F. \quad (16.5)$$

In total, a single motor of a certain motor species is described by six parameters as explained in Figure 16.3. For the plus motor kinesin-1 and the cytoplasmic minus motor dynein, most of these single motor parameters have been determined experimentally; the corresponding parameter values are summarized in Table 16.1 [13]. This theoretical description for a single motor incorporates all results of single molecule experiments that are relevant for large-scale cargo transport.

16.3.4 One Team of Identical Motors

In this section, we consider cargo transport by one team of motors, that is, N motors of the same type are attached to one cargo as shown in Figure 16.4. Since each motor binds to and unbinds from the filament in a stochastic manner, the number n of motors that crosslink the cargo to the filament and thus can actively pull on it varies with time between $n = 0$ and $n = N$ as illustrated in Figure 16.4. The motors are taken to act independently. If n motors are bound to the filament in the absence of load, the unbinding of one of these

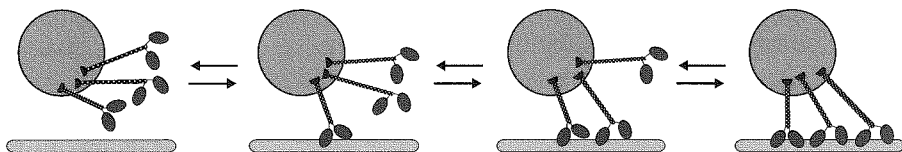


Figure 16.4. Transport by one team of identical motors. Each motor is characterized by a long stalk (grey), by which it is firmly attached to the cargo particle (red), and by two motor heads (blue), which can bind to the filament and then actively pull on the cargo. In this example, the total number of motors is $N = 3$ but the actual number n of crosslinking motors fluctuates between $n = 0$ and $n = 3$ because of thermally induced motor unbinding and rebinding. (See color insert.)

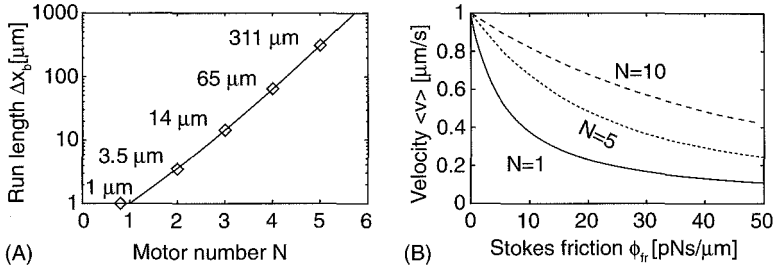


Figure 16.5. Transport by one team of identical motors. (A) The cargo's run length Δx_b increases exponentially with the total number N of motors attached to the cargo. (B) The average cargo velocity $\langle v \rangle$ decreases with increasing friction coefficient ϕ_{fr} , but less so for larger motor number N . The single motor parameters correspond to kinesin-1 as given in Table 16.1.

bound motors is governed by the unbinding rate $n\epsilon_0$, and the rebinding of one of the $N - n$ unbound motors back to the filament takes place with rate $(N - n)\pi_0$ [11].

16.3.4.1 Processivity Enhancement A major problem of cargo transport by a single motor is the motor's finite run length $\Delta x_b \sim 1 \mu\text{m}$, which is too small to cover typical cellular distances of tens of micrometers. Cargo transport by several molecular motors leads to a dramatic increase in the cargo's run length; see Figure 16.5A. Intuitively, if one motor unbinds from the filament, the cargo remains attached to the filament as long as it is still crosslinked by another motor, giving the unbound motor a chance to rebind; compare Figure 16.4. An explicit calculation shows that the average run length Δx_b is given by [11]

$$\Delta x_b = \frac{v_f}{N\pi_0} \left[(1 + \pi_0/\epsilon_0)^N - 1 \right] \quad (16.6)$$

that is, it increases exponentially with the motor number N for large N . If the cargo is transported by kinesin-1 motors, only three such kinesins are required to cross a cell of $10\text{-}\mu\text{m}$ diameter; see Figure 16.5A. The increase of run length with increasing motor number has been observed in vitro [63, 64], but it has been difficult to determine the number of motors pulling the cargo. In recent experiments, the motor number was determined by force measurements [54] or dynamic light scattering [10]. In the latter case, the theory described here was used to describe the data quantitatively.

16.3.4.2 Frictional Forces Another feature of cargo transport by several motors is the ability to sustain large forces arising, for example, from hydrodynamic friction. For a cargo particle of radius $R = 1 \mu\text{m}$ in water with

dynamical viscosity $\eta = 1 \text{ mPa}\cdot\text{s}$, the friction coefficient is $\phi_{\text{fr}} \sim 10^{-2} \text{ pN}\cdot\text{s}/\mu\text{m}$, which does not significantly change the velocity of a cargo particle that is transported by a single motor; see the curve for $N = 1$ in Figure 16.5B. However, as discussed in Section 16.2.2, particle diffusion in the crowded cytoplasm is reduced by a factor of 10–1000 [3], depending on the size of the particle. Since the friction coefficient in Equation 16.1 is inversely proportional to the diffusion constant, the cytoplasmic friction coefficient is 10–1000 times larger than the one in water and leads to a significant reduction of the cargo velocity if the cargo particle is pulled by only one motor; see Figure 16.5B. When the cargo is pulled by $N > 1$ motors, these N motors can share the force, so that the average cargo velocity remains relatively high even for large friction coefficient ϕ_{fr} ; see Figure 16.5B.

16.3.5 Two Teams of Antagonistic Motors

As discussed in Section 16.2.2, many cellular cargoes undergo fast transport both toward the plus end and toward the minus end of the microtubules. This bidirectional transport implies that these cargo particles must be attached to both plus-end and minus-end directed motors.

16.3.5.1 Tug-of-War Between Motors We now consider a cargo particle that is attached to N_+ plus and N_- minus motors. Because each motor unbinds from and rebinds to the filament in a stochastic manner, both the number of active plus motors and the number of active minus motors now fluctuate; see Figure 16.6. Three situations are possible: in the (+) states, only plus motors are active, which can pull the cargo into the plus direction without any opposition from the minus motors; in the (–) states, only minus motors are active and the cargo exhibits fast minus motion; and in the (0) states both types of motors are bound to the filament. In the latter case, the motors pull the cargo into opposite directions, leading to slow cargo movement. Since many bidirectional cargoes are observed to exhibit long periods of fast unidirectional motion, the motors must “cooperate” in some way to avoid the (0) states.

Two mechanisms for bidirectional transport have been proposed [29, 30]: (1) coordination by a putative protein complex, which ensures that only one type of motors is active at any given time; and (2) tug-of-war between the motors that pull on each other until the stronger team wins and determines the direction of motion for a certain period of time. Previously, it was thought that a tug-of-war would lead to a prevalence of (0) states with slow cargo motion and thus would be inconsistent with the experimental observation of fast cargo motion [29, 30]. However, we have developed a realistic tug-of-war model, which is based on the single motor description as presented in Section 16.3.3 as well as on the assumptions that (1) each motor team exerts load forces on the other team and (2) motors of one team share the load force generated by the antagonistic motor team [12, 13]. Such a tug-of-war, which

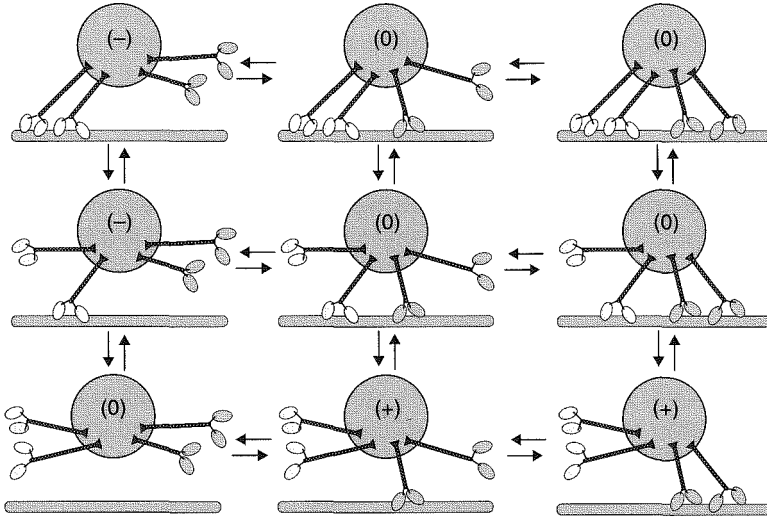


Figure 16.6. Transport by two antagonistic teams of motors. The motors with blue heads are plus motors that pull to the right, the ones with yellow heads are minus motors that pull to the left. Both types of motors are firmly attached to the cargo particle (grey) via their long stalks. The total number of blue plus motors and yellow minus motors is $N_+ = 2$ and $N_- = 2$, respectively. The cargo particle exhibits $(N_+ + 1)(N_- + 1) = 9$ different states and undergoes transitions between these states arising from the unbinding and rebinding of single motors. (See color insert.)

does not require any coordination complex, is consistent with all experimental observations [13, 65].

16.3.5.2 Patterns of Movements As shown in Refs. 12 and 13, a cargo transported by two teams of motors can exhibit different patterns of motility (or “motility states”) depending on the single motor parameters. For the single motor parameters given in Table 16.1, the cargo transport exhibits a dynamic instability, which effectively makes the (0) states very unlikely: if both types of motors are active simultaneously, they exert forces on each other and tend to pull each other off the filament. If, for example, a minus motor unbinds, each of the remaining minus motors has to sustain a larger force arising from the opposing team. Since the unbinding rate in Equation 16.4 increases exponentially with the force, the remaining minus motors now have a high unbinding probability, and undergo an unbinding cascade until all minus motors are detached. A similar unbinding cascade can happen for the plus motors. Because of these unbinding cascades, the cargo is unlikely to stay in a (0) state, in which both types of motors are attached to the filament, but is likely to attain a (+) or (-) state, in which only plus or only minus motors are bound to filament. Therefore the spatial displacement (or trajectory or kymograph) of a cargo pulled by several kinesin-1 and several dynein motors exhibits

alternating periods of fast plus and fast minus motion at speeds of micrometers/second ($\mu\text{m/s}$); see Figure 16.7A. Switching between the two directions happens when a series of motor binding and unbinding events leads to the predominance of the opposing team, which is then stabilized by another unbinding cascade.

16.3.5.3 Advantages for Cargo Transport The tug-of-war performed by two motor species has several advantages for the cell. First, fast bidirectional motion is possible without any coordination complex. Second, cargo transport can easily be regulated, since a change in a single motor parameter affects the competition of the two teams and can lead to net plus or net minus motion by increasing or decreasing the corresponding run lengths, as found experimentally [33–36]. Third, the transport by teams of motors again leads to larger force generation and to enhanced processivity [66]. In particular, the binding time of a cargo increases exponentially with the numbers N_+ and N_- of attached plus and minus motors, respectively. The tug-of-war model described here leads to the binding time Δt_b as given by

$$\Delta t_b(N_+, N_-) \equiv \frac{(1 + \pi_{0+}/\epsilon_{0+})^{N_+} + (1 + \pi_{0-}/\epsilon_{0-})^{N_-} - 2}{N_+ \pi_{0+} + N_- \pi_{0-}} \quad (16.7)$$

where the indices “+” and “-” label plus and minus motor parameters, respectively. Fourth, the stochastic switching of bidirectional transport leads to enhanced diffusion on long time and large length scales; see Figure 16.7B. On short time scales, the cargo particle moves ballistically, that is, the mean square displacement increases quadratically with time, while it increases linearly on long time scales, with a diffusion coefficient of about $1 \mu\text{m}^2/\text{s}$. This diffusion constant is similar to the diffusion constant of a $1\text{-}\mu\text{m}$ sized cargo particle in

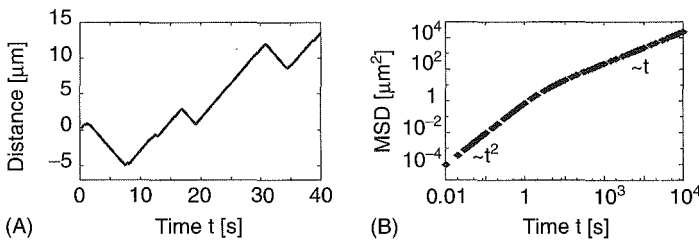


Figure 16.7. Transport by two antagonistic teams of motors. (A) Spatial displacement (or trajectory or kymograph) of cargo particle as a function of time. The cargo is pulled by 4 dyneins and 3 kinesins with single motor parameters as in Table 16.1 and exhibits fast transport in both the plus direction and minus direction. (B) Mean square displacement (MSD) of cargo as a function of time. The cargo is pulled by $N_+ = 4$ plus and $N_- = 4$ minus motors, which are both characterized by kinesin parameters as in Table 16.1. The cargo’s MSD grows quadratically and linearly with time for short and long times, respectively.

water, and about 100–1000 times larger than the diffusion constant of such a particle in the cytoplasm. This enhanced diffusion should be especially useful for cargoes in search of their destination, or for cargo particles such as mitochondria or pigment granules that must be distributed over the whole cell [29, 36, 67]. Finally, one would intuitively expect that bidirectional transport helps to reduce jams in the dense traffic of cargo particles as found in eukaryotic cells. Indeed, if a jam builds up in one direction, for example, because of an obstacle, the cargo particles at the very end of the jam may then move in the opposite direction and, in this way, start to dissolve the jam.

16.3.6 Two Teams of Motors Working on Different Tracks

As discussed in Section 16.2.2, tracks for the long- and short-ranged transport of intracellular cargo particles are provided by microtubules and actin filaments, respectively. In order to switch between these two filament systems without interruptions, many cargo particles are attached to both microtubule- and actin-based motors [38, 39]. The probability of switching between the two filaments depends on the number and types of motors, on the cargo, as well as on cellular regulation [36, 40, 68].

16.3.6.1 Processivity Enhancement During transport on one type of filament, both types of motors may be crosslinked to this filament. Indeed, myosin V, which walks along actin filaments, can also bind to microtubules and diffuse randomly on these latter filaments, whereas kinesin-1, which walks along microtubules, exhibits a weak affinity for actin filaments as well [49, 69]. This type of transport is illustrated in Figure 16.8A for a cargo particle that is

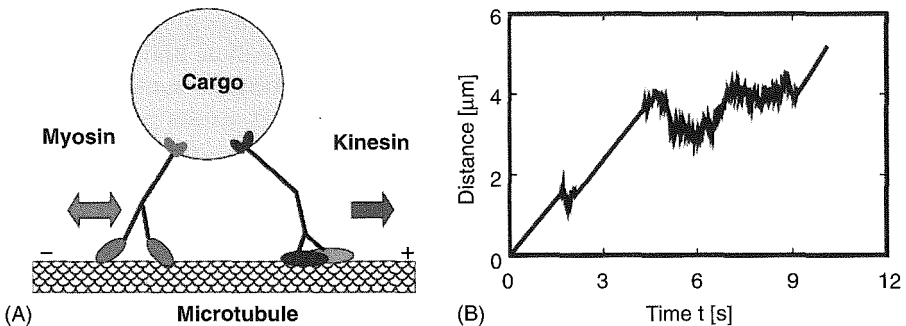


Figure 16.8. Cargo transport by one active and one “passive” motor. (A) A cargo particle (grey) is crosslinked to a microtubule by one kinesin-1 (blue) and one myosin V (red). The kinesin-1 motor is actively stepping whereas the myosin V motor is passively diffusing along the filament. (B) The trajectory of such a cargo exhibits fast plus motion interrupted by diffusive events. For this example, the total binding time was about 11 s, much longer than in the absence of the “passive” myosin V motor [14]. (See color insert.)

crosslinked to a microtubule by both one kinesin-1 motor, which actively walks along the microtubule, and one myosin V, which passively diffuses along this filament. Such a cargo particle exhibits fast plus motion interrupted by diffusive events; see Figure 16.8B. It is then necessary to distinguish the run length, which the cargo particle exhibits during its plus motion, from the binding length of the composite cargo motion.

The binding length of a cargo particle that is transported by one kinesin-1 motor and one myosin V motor is more than two times larger than that of a cargo particle transported by only one kinesin motor [49]. This processivity enhancement can be understood from the single motor properties of kinesin and myosin (compare Section 16.3.3), provided the myosin motor is characterized by its bound diffusion constant rather than by its velocity [14]. The increase in run length arises in a similar way as for cargo transport by a team of identical motors; see Section 16.3.4. If the kinesins unbind, the myosins still act as crosslinkers between cargo and microtubules, thereby preventing the cargo from diffusing away from the filament and giving the kinesins a chance to rebind. Furthermore, in contrast to the competition between kinesin and dynein as described in Section 16.3.5, the simultaneous crosslinking by kinesin-1 and myosin V does not lead to a tug-of-war: because of the relatively weak affinity of myosin V to microtubules, myosin V motors can easily be dragged along by kinesin motors toward the plus end of the microtubule [14].

16.4 CONCLUSION AND DISCUSSION

Cellular cargoes, including endosomes, RNAs, protein complexes, and filaments as well as whole organelles, travel through the cell with the help of molecular motors that pull them along cytoskeletal filaments: kinesin and dynein motors mediate long-ranged transport on microtubule filaments, while local delivery is accomplished by myosin motors walking on a meshwork of actin filaments.

16.4.1 Team Work of Motors

As described in this chapter, molecular motors work in teams in order to meet the challenges of intracellular transport. Three types of teamwork have been identified and elucidated. First, one team of identical motors as shown in Figure 16.4 is able to transport large cargoes through the viscous cytoplasm at considerable speeds of micrometers/second over distances of many micrometers; see Figure 16.5. Second, two teams of antagonistic motors that walk into opposite directions, as in Figure 16.6, accomplish bidirectional transport along an isopolar cytoskeletal network of motor tracks as illustrated in Figure 16.7A. Third, two teams of motors that can walk on different filaments (see

Figure 16.8) allow a smooth transit from the long-range microtubule traffic to the short-range delivery on actin filaments and vice versa. The presence of several motor teams on one cargo allows versatile transport and fast reaction to cellular regulation. A regulation cascade that targets the motor proteins can change the transport properties of the cargo “on the fly,” making it travel on a microtubule to the minus instead of the plus direction by downregulating kinesin, or switching to actin filaments by upregulating myosin.

16.4.2 Virus, Gene, and Drug Delivery

Many viruses hijack the intracellular transport systems and use them for their own purposes. These viruses recruit molecular motors from the host’s cytoplasm and, in addition, “know” how to activate these motors to ensure transport to the desired destination. Copying this viral strategy would dramatically increase the efficiency of gene therapy and drug delivery, because transport through the crowded and viscous cytoplasm would be strongly enhanced. Virus-based expression vectors should include all factors that allow the virus to use the host’s transport machinery during entry and transcription, but not those involved in virus replication and egress. Nonviral vectors and drug carriers should be able to recruit motor proteins from the cytoplasm, for example, by coating them with receptor proteins for molecular motors. Although many of the motor–cargo interactions still remain to be elucidated, an increasing catalog of receptor proteins is emerging [8]. Ideally, the appropriate receptors should be selected from such a catalog in order to bind the correct number and types of motors from the cytoplasm to the gene or drug carrier. The choice of motors should reflect the cargo destination, and possible responses to intracellular or externally applied regulatory stimuli.

16.4.3 Outlook: Open Questions and Possible Applications

In order to construct such carrier and delivery systems, a good understanding of molecular motor traffic is necessary. Although much progress has been made during the last couple of years, many open questions remain. These include the details of the molecular stepping mechanisms of the different motors, the understanding of motor cooperativity, as well as the understanding of overall cellular traffic. A particularly challenging topic is the coupling of motor transport to cellular regulation.

Such an understanding of molecular motor traffic would also be useful for other types of applications in medicine and nanotechnology. One example is provided by antiviral therapies: efficiency of virus infection would be greatly reduced if the viruses were prevented from hijacking the cellular transport machinery in an appropriate way. Likewise, understanding of molecular motor traffic could be useful in order to treat diseases in which improper intracellular transport plays an important role, such as Alzheimer’s disease or lissencephaly

[70, 71]. Finally, molecular motors are possible building blocks for nanotechnological applications. One example is provided by molecular motors that carry cargoes on lab-on-a-chip devices [72, 73].

REFERENCES

1. Cohen, R. N., Rashkin, M. J., Wen, X., and Szoka, F. C. Molecular motors as drug delivery vehicles. *Drug Discov. Today* **2**: 111–118 (2005).
2. Vaughan, E. E., DeGiulio, J. V., and Dean, D. A. Intracellular trafficking of plasmids for gene therapy: mechanisms of cytoplasmic movement and nuclear import. *Curr. Gene Ther.* **6**: 671–681 (2006).
3. Luby-Phelps, K. Cytoarchitecture and physical properties of cytoplasm: volume, viscosity, diffusion, intracellular surface area. *Int. Rev. Cytol. Surv. Cell Biol.* **192**: 189–221 (2000).
4. Lukacs, G. L., Haggie, P., Seksek, O., Lechardeur, D., Freedman, N., and Verkman, A. S. Size-dependent DNA mobility in cytoplasm and nucleus. *J. Biol. Chem.* **275**: 1625–1629 (2000).
5. Dowty, M. E., Williams, P., Zhang, G. F., Hagstrom, J. E., and Wolf, J. A. Plasmid DNA entry into postmitotic nuclei of primary rat myotubes. *Proc. Natl. Acad. Sci. U.S.A.* **92**: 4572–4576 (1995).
6. Capecchi, M. R. High-efficiency transformation by direct micro-injection of DNA into cultured mammalian-cells. *Cell* **22**: 479–488 (1980).
7. Campbell, E. M. and Hope, T. J. Gene therapy progress and prospects: viral trafficking during infection. *Gene Ther.* **12**: 1353–1359 (2005).
8. Dohner, K., Nagel, C. H., and Sodeik, B. Viral stop-and-go along microtubules: taking a ride with dynein and kinesins. *Trends Microbiol.* **13**: 320–327 (2005).
9. Greber, U. F. and Way, M. A superhighway to virus infection. *Cell* **124**: 741–754 (2006).
10. Beeg, J., Klumpp, S., Dimova, R., Gracià, R. S., Unger, E., and Lipowsky, R. Transport of beads by several kinesin motors. *Biophys. J.* **94**: 532–541 (2008).
11. Klumpp, S. and Lipowsky, R. Cooperative cargo transport by several molecular motors. *Proc. Natl. Acad. Sci. U.S.A.* **102**: 17284–17289 (2005).
12. Müller, M. J. I., Klumpp, S., and Lipowsky, R. Motility states of molecular motors engaged in a stochastic tug-of-war. *J. Stat. Phys.* **133**: 1059–1081 (2008).
13. Müller, M. J. I., Klumpp, S., and Lipowsky, R. Tug-of-war as a cooperative mechanism for bi-directional cargo transport by molecular motor. *Proc. Natl. Acad. Sci. U.S.A.* **105**: 4609–4614 (2008).
14. Berger, F., Müller, M. J. I., and Lipowsky, R. Enhancement of the processivity of kinesin-transported cargo by myosin V. *EPL* **87**: 28002 (2009).
15. Alberts, B., Bray, D., Johnson, A., Lewis, J., Raff, M., Roberts, K., and Walter, P. *Essential Cell Biology. An Introduction to the Molecular Biology of the Cell.* Garland, New York, 1998.
16. Brady, S. T. A novel brain ATPase with properties expected for the fast axonal transport motor. *Nature* **317**: 73–75 (1985).

17. Vale, R. D., Reese, T. S., and Sheetz, M. P. Identification of a novel force-generating protein, kinesin, involved in microtubule-based motility. *Cell* **42**: 39–50 (1985).
18. Vale, R. D. The molecular motor toolbox for intracellular transport. *Cell* **112**: 467–480 (2003).
19. Block, S. M. Kinesin motor mechanics: binding, stepping, tracking, gating, and limping. *Biophys. J.* **92**: 2986 (2007).
20. Paschal, B. M., Sheptner, H. S., and Vallee, R. B. MAP-1C is a microtubule-activated ATPase which translocates microtubules invitro and has dynein-like properties. *J. Cell Biol.* **1057**: 1273–1282 (1987).
21. Gennerich, A. and Vale, R. D. Walking the walk: how kinesin and dynein coordinate their steps. *Curr. Opin. Cell Biol.* **21**: 59–67 (2009).
22. Howard, J. *Mechanics of Motor Proteins and the Cytoskeleton*. Sinauer Associates, Sunderland, MA, 2001.
23. Mallik, R. and Gross, S. P. Molecular motors: strategies to get along. *Curr. Biol.* **14**: R971–R982 (2004).
24. Goldstein, L. S. B. and Yang, Z. Microtubule-based transport systems in neurons: the roles of kinesins and dyneins. *Annu. Rev. Neurosci.* **23**: 39–71 (2000).
25. Carter, N. J. and Cross, R. A. Mechanics of the kinesin step. *Nature* **435**: 308–312 (2005).
26. Toba, S., Watanabe, T. M., Yamaguchi-Okimoto, L., Toyoshima, Y. Y., and Higuchi, H. Overlapping hand-over-hand mechanism of single molecular motility of cytoplasmic dynein. *Proc. Natl. Acad. Sci. U.S.A.* **103**: 5741–5745 (2006).
27. Gross, S. P., Vershinin, M., and Shubeita, G. T. Cargo transport: two motors are sometimes better than one. *Curr. Biol.* **17**: R478–R486 (2007).
28. Lane, J. and Allan, V. Microtubule-based membrane movement. *Biochim. Biophys. Acta* **1376**: 27–55 (1998).
29. Gross, S. P. Hither and yon: a review of bi-directional microtubule-based transport. *Phys. Biol.* **1**: R1–R11 (2004).
30. Welte, M. A. Bi-directional transport along microtubules. *Curr. Biol.* **14**: R525–R537 (2004).
31. Klumpp, S., Nieuwenhuizen, Th. M., and Lipowsky, R. Self-organized density patterns of molecular motors in arrays of cytoskeletal filaments. *Biophys. J.* **88**: 3118–3132 (2005).
32. Müller, M. J. I., Klumpp, S., and Lipowsky, R. Molecular motor traffic in a half-open tube. *J. Phys. Condens. Matter* **17**: S3839–S3850 (2005).
33. Morris, N. R. and Hollenbeck, P. J. The regulation of bi-directional mitochondrial transport is coordinated with axonal outgrowth. *J. Cell Sci.* **104**: 917–927 (1993).
34. Gross, S. P., Welte, M. A., Block, S. M., and Wieschaus, E. F. Dynein-mediated cargo transport in vivo: a switch controls travel distance. *J. Cell Biol.* **148**: 945–955 (2000).
35. Smith, G. A., Murphy, B. J., Gross, S. P., and Enquist, L. W. Local modulation of plus-end transport targets herpesvirus entry and egress in sensory axons. *Proc. Natl. Acad. Sci. U.S.A.* **101**: 16034–16039 (2004).
36. Gross, S. P., Tuma, M. C., Deacon, S. W., Serpinskaya, A. S., Reilein, A. R., and Gelfand, V. I. Interactions and regulation of molecular motors in *Xenopus* melanophores. *J. Cell Biol.* **156**: 855–865 (2002).

37. Tuma, M. C. and Gelfand, V. I. Molecular mechanisms of pigment transport in melanophores. *Pigment Cell Res.* **12**: 283–294 (1999).
38. Brown, S. S. Cooperation between microtubule- and actin-based motor proteins. *Annu. Rev. Cell Dev. Biol.* **15**: 63–80 (1999).
39. Goode, B. L., Drubin, D. G., and Barnes, G. Functional cooperation between the microtubule and actin cytoskeletons. *Curr. Opin. Cell Biol.* **12**: 63–71 (2000).
40. Snider, J., Lin, F., Zahedi, N., Rodionov, V., Yu, C. C., and Gross, S. P. Intracellular actin-based transport: How far you go depends on how often you switch. *Proc. Natl. Acad. Sci. U.S.A.* **101**: 13204–13209 (2004).
41. Lipowsky, R. and Klumpp, S. “Life is motion”—multiscale motility of molecular motors. *Physica A* **352**: 53–112 (2005).
42. Liepelt, S. and Lipowsky, R. Kinesin’s network of chemomechanical motor cycles. *Phys. Rev. Lett.* **98**: 258102 (2007).
43. Lipowsky, R., Klumpp, S., and Nieuwenhuizen, Th. M. Random walks of cytoskeletal motors in open and closed compartments. *Phys. Rev. Lett.* **87**: 108101 (2001).
44. Maly, I. V. A stochastic model for patterning of the cytoplasm by the salutatory movement. *J. Theor. Biol.* **216**: 59–71 (2002).
45. Parmeggiani, A., Franosch, T., and Frey, E. Phase coexistence in driven one dimensional transport. *Phys. Rev. Lett.* **90**: 086601 (2003).
46. Smith, D. A. and Simmons, R. M. Models of motor-assisted transport of intracellular particles. *Biophys. J.* **80**: 45–68 (2001).
47. Kuznetsov, A. V., Avramenko, A. A., and Blinov, D. G. Numerical modeling of molecular-motor-assisted transport of adenoviral vectors in a spherical cell. *Comput. Methods Biomech. Biomed. Eng.* **11**: 215–222 (2008).
48. Lagache, T., Dauty, E., and Holcman, D. Quantitative analysis of virus and plasmid trafficking in cells. *Phys. Rev. E* **79**: 011921 (2009).
49. Ali, M. Y., Lu, H., Bookwalter, C. S., Warshaw, D. M., and Trybus, K. M. Myosin V and kinesin act as tethers to enhance each others’ processivity. *Proc. Natl. Acad. Sci. U.S.A.* **105**: 4691–4696 (2008).
50. Campàs, O., Leduc, C., Bassereau, P., Casademunt, J., Joanny, J.-F., and Prost, J. Coordination of kinesin motors pulling on fluid membranes. *Biophys. J.* **94**: 5009–5017 (2008).
51. Diehl, M. R., Zhang, K., Lee, H. J., and Tirrell, D. A. Engineering cooperativity in biomotor protein assembly. *Science* **311**: 1468–1471 (2006).
52. Leduc, C., Campàs, O., Zeldovich, K. B., Roux, A., Jolimaitre, P., Bourel, L., Bonnet, B. G., Joanny, J.-F., Bassereau, P., and Prost, J. Cooperative extraction of membrane nanotubes by molecular motors. *Proc. Natl. Acad. Sci. U.S.A.* **101**: 17096–17101 (2004).
53. Leduc, C., Ruhnnow, F., Howard, J., and Diez, S. Detection of fractional steps in cargo movement by the collective operation of kinesin-1 motors. *Proc. Natl. Acad. Sci. U.S.A.* **104**: 10847–10852 (2007).
54. Vershinin, M., Carter, B. C., Razafsky, D. S., King, S. J., and Gross, S. P. Multiple-motor based transport and its regulation by Tau. *Proc. Natl. Acad. Sci. U.S.A.* **104**: 87–92 (2007).
55. Badoual, M., Jülicher, F., and Prost, J. Bi-directional cooperative motion of molecular motors. *Proc. Natl. Acad. Sci. U.S.A.* **99**: 6696–6701 (2002).

56. Kunwar, A., Vershinin, M., Xu, J., and Gross, S. P. Stepping, strain gating, and an unexpected force-velocity curve for multiple-motor-based transport. *Curr. Biol.* **18**: 1–11 (2008).
57. Nishiyama, M., Higuchi, H., and Yanagida, T. Chemomechanical coupling of the forward and backward steps of single kinesin molecules. *Nat. Cell Biol.* **4**: 790–797 (2002).
58. Visscher, K., Schnitzer, M. J., and Block, S. M. Single kinesin molecules studied with a molecular force clamp. *Nature* **400**: 184–189 (1999).
59. Schnitzer, M. J., Visscher, K., and Block, S. M. Force production by single kinesin motors. *Nat. Cell Biol.* **2**: 718–723 (2000).
60. King, S. J. and Schroer, T. A. Dynactin increases the processivity of the cytoplasmic dynein motor. *Nat. Cell Biol.* **2**: 20–24 (2000).
61. Kramers, H. A. Brownian motion in a field of force and the diffusion model of chemical reactions. *Physica* **7**: 284–304 (1940).
62. Bell, G. I. Models for the specific adhesion of cells to cells. *Science* **200**: 618–627 (1978).
63. Block, S. M., Goldstein, L. S. B., and Schnapp, B. J. Bead movement by single kinesin molecules studied with optical tweezers. *Nature* **348**: 345–352 (1990).
64. Coy, D. L., Wagenbach, M., and Howard, J. Kinesin takes one 8-nm step for each ATP that it hydrolyzes. *J. Biol. Chem.* **274**: 3667–3671 (1999).
65. Welte, M. A. and Gross, S. P. Molecular motors: a traffic cop within? *HFSP J.* **2**: 178–182 (2008).
66. Müller, M. J. I., Klumpp, S., and Lipowsky, R. Dynamics of bi-directional transport by molecular motors. *Biophys. J.* **98**: 2610–2618 (2010).
67. De Vos, K. J., Sable, J., Miller, K. E., and Sheetz, M. P. Expression of phosphatidylinositol(4,5) biphosphate-specific pleckstrin homology domains alters direction but not the level of axonal transport of mitochondria. *Mol. Biol. Cell* **14**: 3636–3649 (2003).
68. Ross, J. L., Ali, M. Y., and Warshaw, D. M. Cargo transport: molecular motors navigate a complex cytoskeleton. *Curr. Opin. Cell Biol.* **20**: 41–47 (2008).
69. Ali, M. Y., Krementsova, E. B., Kennedy, G. G., Mahafy, R., Pollard, T. D., Trybus, K. M., and Warshaw, D. M. Myosin Va maneuvers through actin intersections and diffuses along microtubules. *Proc. Natl. Acad. Sci. U.S.A.* **104**: 4332–4336 (2007).
70. Aridor, M. and Hannan, L. A. Traffic jams II: an update of diseases of intracellular transport. *Traffic* **3**: 781–790 (2002).
71. Duncan, J. E. and Goldstein, L. S. The genetics of axonal transport and axonal transport disorders. *PLoS Genet.* **2**: e124 (2006).
72. Hess, H., Bachand, G. D., and Vogel, V. Powering nanodevices with biomolecular motors. *Chem. Eur. J.* **10**: 2110–2116 (2004).
73. van den Heuvel, M. G. L. and Dekker, C. Motor proteins at work for nanotechnology. *Science* **317**: 333–336 (2007).